# Equilibrium, kinetic and structural properties of gallium(III)- and some divalent metal complexes formed with the new DATAm and DATA5m ligands

Edit Farkas,[a] Johannes Nagel,[b] Alessandro Maiocchi,[c] Bradley P. Waldron,[d] David Parker,[d] Imre Tóth,[a] Ernő Brücher,[a] Frank Roesch*[b] and Zsolt Baranyai*[a,c]

**Abstract:** The development of $^{68}$Ge/$^{68}$Ga generators has made the positron emitting $^{68}$Ga isotope widely accessible, raising interest in new chelate complexes of $Ga^{3+}$. The hexadentate DATAm ligand and its bifunctional analogue, DATA5m, rapidly form complexes with $^{68}$Ga in high radiochemical yield. The stability constants of DATAm and DATA5m complexes formed with $Ga^{3+}$, $Zn^{2+}$, $Cu^{2+}$, $Mn^{2+}$ and $Ca^{2+}$ have been determined by pH-potentiometry, spectrophotometry ($Cu^{2+}$) and $^1$H- and $^{71}$Ga-NMR spectroscopy ($Ga^{3+}$). The stability constants of Ga(DATAm) and Ga(DATA5m) complexes are higher than those of the Ga(AAZTA). The species distribution calculations indicate the predominance of Ga(L)OH mixed hydroxo complexes at physiological pH. The $^1$H- and $^{71}$Ga-NMR studies provided information about the coordinated functional groups of ligands and on the kinetics of exchange between the Ga(L) and Ga(L)OH complexes. The transmetallation reactions between the Ga(L) complexes and $Cu^{2+}$-citrate ($6 < pH < 8.5$) occur through both spontaneous and OH$^-$ assisted dissociation of the Ga(L)OH species. At pH = 7.4 and 25°C, the half lives of the dissociation of Ga(DATAm), Ga(DATA5m) and Ga(AAZTA) are 11 h, 44 h and 24 h, respectively. Similar half-lives have been obtained for the ligand exchange reactions between the Ga(L)OH complexes and transferrin. The equilibrium and kinetic data indicate that the Ga(DATA5m) complex is a good candidate as a $^{68}$Ga-based radiodiagnostic.

## Introduction

The visualization of biological processes at the molecular level and their qualitative and quantitative assessment is the domain of Molecular Imaging (MI). The established diagnostic power of the Positron Emission Tomography (PET) technique in MI and the increasing availability of new biological targeting vectors have led to the design and testing of a large number of radiopharmaceuticals in oncology, cardiology, neurology, and infectious diseases.[1] The introduction of radionuclides like $^3$H, $^{11}$C or $^{18}$F to biological targeting vectors needs time consuming synthesis. Taking the half-life of these nuclides into account, this

is the main disadvantage for these radioisotopes in means of preparation and examination of their derivatives. Radiometal ions, instead, can be complexed in a single step to yield the desired product. These probes can be used for diagnosis via PET or SPECT imaging.[2] The major concern for most radionuclides is their availability and their means of production. Therefore, the use of generator produced isotopes has become of great interest over the last few years.[3] The widespread clinical application of $^{68}$Ge-based radioisotope generators ($t_{1/2}$ ($^{68}$Ge)=270.8 days) for the production of the PET isotope $^{68}$Ga ($t_{1/2}$ = 67.71 min, $E_{\beta+,max}$=1.89 MeV, 89% decays through positron emission), together with its favourable properties, *i.e.* half-life sufficient for production and application of tracers with relatively low radiation dose to the patient, has gained the research activity for the development of effective, specific and safe $^{68}$Ga-based radiopharmaceuticals.[4,5] Because of the similar properties of $Ga^{3+}$ and $Fe^{3+}$ -ions, the $^{68}$Ga-based radiopharmaceutical consists of a thermodynamically stable and kinetically inert Ga$^{III}$ -complex linked to a specific vector, most often represented by peptides or pseudo-peptides. The $Ga^{3+}$ ion is known to form stable complexes with carboxylate, hydroxamate, phenolate, but will also bind well to "softer" amine and thiolate groups. The coordination of $Ga^{3+}$ with several different ligands has been thoroughly investigated, starting from the screening work of Martell[6] and followed, in the last two decades, by the design and development of novel and improved Ga$^{III}$-complexes in order to prevent the transmetallation reaction with endogeneous metal ions ($Cu^{2+}$, $Zn^{2+}$, $Ca^{2+}$) or transchelation reactions with proteins such as transferrin.[7] It is well established that macrocyclic chelators such as 1,4,7,10-tetraazacyclododecane-1,4,7,10-tetraacetic acid (DOTA) and 1,4,7-triazacyclononane-1,4,7-triacetic acid (NOTA), either free or conjugated to peptides, form thermodynamically stable and kinetically inert complexes with $^{68}$Ga.[7-9] However, the efficient labeling of DOTA and NOTA ligands with $^{68}$Ga isotope requires a large excess of ligand (>1000 fold) and high temperature (95°C) which tend to denature the biologically active proteins. In this context, there is intensive search for highly $Ga^{3+}$ specific chelators for efficient $^{68}$Ga-labeling at room temperature.[9]

The heptadentate ligand AAZTA (Scheme 1) is easily prepared.[10] Its coordination properties towards a wide array of metal ions have been reported, showing its remarkable affinities to lanthanides and transition metal ions.[11-14] The ready availability of AAZTA and recent descriptions of its lipophilic derivatives for targeting high density lipoproteins (HDL),[15] cell membranes,[16] the synthesis of bifunctional compounds for conjugation purposes,[17] and the fast formation of complexes prompted us to explore the possibility of employing the AAZTA platform for developing useful complexes for targeted PET applications.[18] Based on the 6-amino-1,4-diazapine (DATA)

[a]    E. Farkas, Prof. I. Tóth, Prof. E. Brücher, Dr. Zs. Baranyai,
        Department of Inorganic and Analytical Chemistry, University of
        Debrecen, H-4032, Debrecen, Egyetem tér 1., Hungary
[b]    J. Nagel, Prof. F. Rösch, Institute of Nuclear Chemistry, University
        of Mainz, Fritz-Strassmann-Weg 2, 55128 Mainz, Germany, E-mail:
        frank.roesch@uni-mainz.de
[c]    Dr. A. Maiocchi, Dr. F. Uggeri, Dr. Zs. Baranyai, Bracco Imaging
        spa, Bracco Research Centre, Via Ribes 5, 10010 Colleretto
        Giacosa (TO), Italy. E-mail: zsolt.baranyai@bracco.com
[d]    Dr. B. P. Waldron, Prof. D. Parker, Department of Chemistry,
        Durham University, South Road, Durham, DH1 3LE, UK

        Supporting information for this article is given via a link at the end of
        the document.

scaffold new hexadentate chelators were developed by Waldron et al that shows favourable complexation behaviour[19,20]
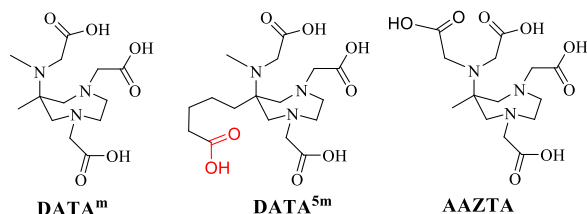


**Scheme 1.** Structure of AAZTA, DATA$^m$ and DATA$^{5m}$ ligands

Radiolabeling experiments with ^{68}Ga of these ligands showed high radiochemical yields after 1 minute and high stability in the first *in vitro* and *in vivo* studies.[21] In this study we synthesized the DATA$^m$ and DATA$^{5m}$ ligands via a new synthesis route and evaluated their protonation behaviour and complex-forming properties with various alkaline earth, transition metal and Ga$^{3+}$ ions. The kinetic inertness of Ga(DATA$^m$) and Ga(DATA$^{5m}$) complexes was investigated via the exchange reactions with Cu$^{2+}$ and transferrin under near physiological conditions. The solution structures and dynamics of the Ga(DATA$^m$) and Ga(DATA$^{5m}$) complexes have also been investigated by $^1$H NMR spectroscopy.

## Results and Discussion

The H$_3$DATA$^m$ and H$_4$DATA$^{5m}$ ligands is a derivative of H$_4$AAZTA in which one of the carboxylate groups is substituted by a methyl group in the imino-diacetate (IMDA) moiety (Scheme 1). In the complexes of AAZTA, three N- and four carboxylate O-atoms can simultaneously bind the metal ion.[11-13] Removing one carboxylate group will evidently affect the equilibrium, kinetic and structural properties of the metal complexes formed with DATA$^m$ and DATA$^{5m}$ ligands. Indeed, the DATA$^m$ ligand has been shown to form a well-defined octahedral Ga(III) complex by X-ray crystallography.[20] Moreover, the presence of the n-valeric acid pendant used for the conjugation of DATA$^{5m}$ to biologically active molecules may influence the physicochemical properties of the metal-complexes. Taking into account these considerations, the behaviour of DATA$^m$ and DATA$^{5m}$ has been compared in detail.

### Solution equilibria of the DATA$^m$ and DATA$^{5m}$ ligands and its complexes

*Protonation equilibria of the H$_3$DATA$^m$ and H$_4$DATA$^{5m}$ ligands*: The protonation constants of the ligands, defined by Eq. (1), have been determined by pH-potentiometry and the log$K_i^H$ values are listed in Table 1. (standard deviations are shown in parentheses). The charges of the ligands and complexes will be used only when it is really necessary.

$$K_i^H = \frac{[H_iL]}{[H_{i-1}L][H^+]}$$ (1)

where i=1, 2...5.

**Table 1.** Protonation constants of DATA$^m$, DATA5$^m$ and AAZTA ligand (0.15 M NaCl, 25°C)

| | DATA$^m$ | MeAAZ3A [a] | DATA$^{5m}$ | AAZTA[b] |
|---|---|---|---|---|
| log$K_1^H$ | 11.27 (1) | 10.90 | 11.39 (1) | 10.06 |
| log$K_2^H$ | 5.15 (2) | 5.14 | 5.30 (2) | 6.50 |
| log$K_3^H$ | 3.49 (1) | 3.71 | 4.35 (2) -COOH | 3.77 |
| log$K_4^H$ | 2.08 (2) | 2.17 | 3.45 (2) | 2.33 |
| log$K_5^H$ | – | – | 2.28 (4) | 1.51 |
| $\Sigma$log$K_i^H$ | 21.99 | 21.92 | 26.77 / 22.42 [c] | 24.17 |

[a] Ref. [22] (MeAAZ3A=DATA$^m$); [b] Ref. [12]; [c] The protonation constant of n-valeric acid is not considered (due to the negligible role in metal binding).

The protonation sequence of the AAZTA ligand was determined by a study of the pH-dependence of the $^1$H-NMR chemical shifts of non-labile protons.[11] The first protonation takes place at the nitrogen atoms of the ring and the pendant arm (the protonation occurs partially at a ring N- and at the imino-diacetate N-atom). The second protonation occurs at the ring nitrogen whereas the first proton is transferred to the nitrogen of the IMDA group because of the electrostatic repulsion between the protonated ring and the exocyclic nitrogen. Further protonations occur at one of the ring-carboxylate groups and non-protonated ring nitrogen atom and/or the carboxylate pendant arms, respectively. According to the $\Delta\delta_H$ values of the non-labile protons of the DATA$^m$ ligand published by Waldron et al.[19] the protonation scheme of DATA$^m$ and DATA$^{5m}$ ligands is very similar to that of AAZTA. A comparison of the protonation constants (Table 1) indicates that log$K_1^H$ and log$K_2^H$ values of DATA$^{5m}$ are slightly higher, whereas the log$K_3^H$ value for DATA$^{5m}$ is 0.7 logK unit higher than for DATA$^m$. The higher log$K_1^H$ and log$K_2^H$ values of DATA$^{5m}$ can be explained by differential solvation of the protonated ligand following introduction of the n-valeric acid moiety.

By considering the protonation constant of n-valeric acid (log$K_1^H$=4.69),[23] it is reasonable to assume that the third protonation of DATA$^{5m}$ involves the carboxylate group of the n-valeric acid pendant. Finally, the log$K_3^H$ and log$K_4^H$ values of DATA$^m$ and log$K_4^H$ and log$K_5^H$ values of DATA$^{5m}$, corresponding to the protonation of the ring-carboxylate and non-protonated ring nitrogen or carboxylate groups, are very similar. It is worth noting that the log$K_1^H$ value of DATA$^m$ and DATA$^{5m}$ is significantly higher than that of the AAZTA ligand, which can be explained by the formation of Na(AAZTA)$^{3-}$ complex competing with the first protonation process. The lower affinity of DATA$^m$ and DATA$^{5m}$ towards Na$^+$ may be related to the absence of one acetate arm on the exocyclic nitrogen, which induces higher flexibility for the coordination cage.

*Complexation properties with M$^{2+}$ cations:* The stability and protonation constants of the metal complexes are defined by Eqs. (2) and (3).

$$K_{ML} = \frac{[ML]}{[M][L]} \qquad (2)$$

$$K_{MH_iL} = \frac{[MH_iL]}{[MH_{i-1}L][H^+]} \qquad (3)$$

where i=1 – 3. The protonation and stability constants of the DATA$^m$ and DATA$^{5m}$ complexes have been calculated from the titration curves obtained at 1:1 metal to ligand concentration ratios. The best fitting was obtained by using a model which includes the formation of *ML*, *MHL*, *MH₂L* and *MH₃L* species in equilibrium. The titration data of the DATA$^m$ and DATA$^{5m}$ in the presence of Zn$^{2+}$ and Cu$^{2+}$ indicate base consuming processes at pH>9. These processes can be interpreted by assuming the hydrolysis of the metal ion; the coordination of OH$^-$ ion results in the formation of M(L)OH species. The protonation of the M(L)OH species can be characterized by the equilibrium constant K$_{MLH-1}$ (Eq (4)).

$$M(L)OH^- + H^+ \rightleftharpoons ML + H_2O \qquad (4)$$
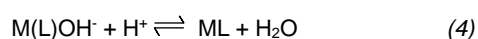
$$K_{MLH_{-1}} = \frac{[ML]}{[M(L)OH^-][H^+]}$$

Because of the high stability of the Cu(DATA$^m$) and Cu(DATA$^{5m}$) complex, the determination of the stability constants cannot be carried out by direct pH-potentiometry. However, it is possible by spectrophotometry. The stability constant has been determined by studying the equilibrium in the Cu$^{2+}$-DATA$^m$-H$^+$ and Cu$^{2+}$-DATA$^{5m}$-H$^+$ systems with UV-Vis spectrophotometry. The competition reaction (Eq. (5)) has been studied in the [H$^+$] range 0.01 – 1.0 M where the species Cu$^{2+}$, Cu(H₃L), Cu(H₂L) and Cu(HL) are present in the equilibria.

$$Cu^{2+} + H_xL \rightleftharpoons Cu(H_yL) + (x-y)H^+ \qquad (5)$$
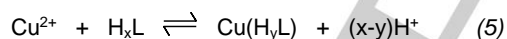
where x = 3 - 4 and y=1 – 2 for DATA$^m$ and x=4 - 5 and y=2 – 3 for DATA$^{5m}$. Some characteristic absorption spectra obtained for the Cu$^{2+}$-DATA$^m$-H$^+$ and Cu$^{2+}$-DATA$^{5m}$-H$^+$ systems are shown in Figure 1.
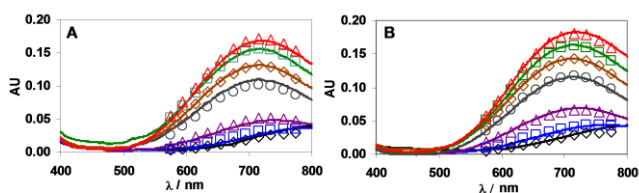


**Figure 1.** The absorption spectra of the Cu$^{2+}$-DATA$^m$-H$^+$ (**A**) and Cu$^{2+}$-DATA$^{5m}$-H$^+$ (**B**) systems as a function of [H$^+$]. The curves and the open symbols represent the experimental and the calculated absorbance values, respectively. ([H$^+$] = **1.0** (◇), **0.60** (□), **0.32** (△), **0.10** (○), **0.05** (◇), **0.025** (□) and **0.01** M (△); [Cu$^{2+}$] = [DATA$^m$] = [DATA$^{5m}$]=0.002 M, [H$^+$]≤0.15 M→[Na$^+$]+[H$^+$]=0.15 M, 25°C, l=1 cm).

The stability constants obtained by pH-potentiometric titration and by UV-Vis spectrophotometric technique for the Cu$^{2+}$ are presented in Table 2. The stability constants of Ca$^{II}$-, Mn$^{II}$- and

Cu$^{II}$-complexes formed with DATA$^m$ and DATA$^{5m}$ ligands are lower by 2 - 3 logK units than those of the corresponding AAZTA complexes. Interestingly, the stability constants of Zn(DATA$^m$) and Zn(DATA$^{5m}$) complexes are higher than that of Zn(AAZTA). A comparison of the logK$_{ML}$ values of metal complexes formed with DATA$^m$ and DATA$^{5m}$ indicates that the stability constants of the DATA$^{5m}$ complexes (Table 2) are generally higher by 0.2 - 0.5 logK units than those of the corresponding complexes of DATA$^m$.

**Table 1.** Stability and protonation constants of DATA$^m$, DATA$^{5m}$ and AAZTA complexes formed with Ca$^{2+}$, Mn$^{2+}$, Zn$^{2+}$ and Cu$^{2+}$ ions (0.15 M NaCl, 25°C)

|  | DATA$^m$ | DATA5$^m$ | AAZTA[a] |
|---|---|---|---|
| CaL | 8.70 (2) | 9.09 (2) | 11.75 (1) |
| CaHL | 5.49 (4) | 5.64 (5) | 3.41 (3) |
| CaH₂L | – | 4.71 (5) | – |
| MnL | 11.43 [b] | 11.63 (2) | 14.19 [b] |
| MnHL | 3.36 [b] | 4.86 (1) | 2.61 [b] |
| MnH₂L | – | 3.53 (4) | – |
| ZnL | 16.54 (2) | 16.91 (2) | 16.02 (1) |
| ZnHL | 1.76 (5) | 4.77 (1) | 3.95 (1) |
| ZnH₂L | – | 1.77 (5) | 2.53 (1) |
| Zn(L)OH | 11.94 (4) | 12.00 (5) | 11.36 (2) |
| CuL[c] | 18.36 (4) | 18.97 (2) | 20.71 |
| CuHL | 3.56 (2) | 4.58 (1) | 3.92 |
| CuH₂L | 1.52 (2) | 3.35 (1) | 2.68 |
| CuH₃L | – | 1.34 (2) | 0.92 |
| Cu(L)OH | 10.88 (1) | 11.10 (4) | 10.79 |

[a] Ref. [12]; [b] Ref. [22]; [c] Spectrophotometry, [H+]=0.01 – 3.0 M, I=[H+]+[Na+]=0.15 M in samples at [H+]<0.15 M.

The complexes formed with the DATA$^m$ and DATA$^{5m}$, similarly to those of AAZTA, can be protonated at lower pH values and the protonation constants have been determined by pH-potentiometry (Table 2). The logK$_{MHL}$ value of Mn$^{II}$, Zn$^{II}$- and Cu$^{II}$-, and the logK$_{MH2L}$ value of Ca$^{II}$-complexes formed with DATA$^{5m}$ are very similar to the logK$_3^H$ value of the free ligand, DATA$^{5m}$. These findings clearly indicate that the n-valeric acid fragment of DATA$^{5m}$ does not participate in the coordination of metal ions, so it can protonate/deprotonate independently. For the complexes formed with Zn$^{2+}$ and Cu$^{2+}$ ions one and two lower protonation constants could be determined, respectively. In these complexes there exists probably one weakly-coordinated donor atoms (a carboxylate-O), which can be protonated in the pH range 2 – 5.

*Equilibrium properties of Ga$^{3+}$-DATA$^m$ and Ga$^{3+}$-DATA$^{5m}$ systems:* The stability and protonation constants of Ga(DATA$^m$) and Ga(DATA$^{5m}$), defined by Eqs. (2) and (3), were determined

by pH-potentiometric titration of solutions from basic to acidic conditions by following the competition between the OH⁻ ions and the DATA$^m$ or DATA$^{5m}$ ligands for Ga$^{3+}$ at high pH values (pH>8), as described in Eq. (6). For the calculations the hydrolysis constants of the free Ga$^{3+}$ ion (log$K_{[Ga(OH)]2+}$ = -2.97, log$K_{[Ga(OH)2]+}$ = -5.92, log$K_{[Ga(OH)3]}$ = -8.2 and log$K_{[Ga(OH)4]-}$ = -17.3) were also used.[24-26]

$$GaL + 4OH^- \rightleftharpoons [Ga(OH)_4]^- + H_xL \qquad (6)$$

The protonation constants of Ga(DATA$^m$) and Ga(DATA$^{5m}$) have been calculated from the titration curves obtained at 1:1 metal to ligand concentration ratios by titrating the preformed complex with standardized HCl solution. The titration data obtained for Ga(DATA$^m$) and Ga(DATA$^{5m}$) at 8>pH>5 indicated the occurrence of an extra acid consuming process. This process can be interpreted by the reaction of a H$^+$ ion with the [Ga(L)OH] species. The formation and protonation of mixed hydroxo [Ga(L)OH] complexes could be characterised by Equations (4) and (7):
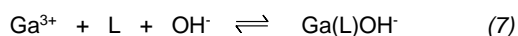
$$Ga^{3+} + L + OH^- \rightleftharpoons Ga(L)OH^- \qquad (7)$$

$$\beta_{GaLH_{-1}} = \frac{[Ga(L)OH]}{[Ga^{3+}][L][OH^-]}$$

The Ga$^{3+}$- DATA$^m$ and Ga$^{3+}$- DATA$^{5m}$ equilibrium systems have also been investigated by $^1$H- and $^{71}$Ga-NMR spectroscopy. The $^1$H- and $^{71}$Ga-NMR spectra of the Ga$^{3+}$- DATA$^m$ and Ga$^{3+}$- DATA$^{5m}$ systems obtained in the pH range 1.5-12.5 are presented in Figures 2 and 3, S1 and S2, respectively. The $^1$H- and $^{71}$Ga-NMR data have also been used to calculate the stability and protonation constants of Ga(DATA$^m$) and Ga(DATA$^{5m}$) complexes by taking into account the integrals of the $^1$H- (Ga(DATA$^m$): C**H$_3$**-C- (1.0 ppm), C**H$_3$**-N- (2.3 ppm), see Figure 2; Ga(DATA$^{5m}$): C**H$_3$**-N- (2.35 ppm), see Figure S1; and $^{71}$Ga-NMR signals of ([Ga(OH)$_4$]$^-$ (223 ppm), see Figures 3 and S2). Moreover, the protonation constant of the n-valeric acid fragment in the Ga(DATA$^{5m}$) complex has also been calculated from the chemical shift variation of the triplet resonance, -C**H$_2$**-COO$^-$, (2.2 ppm), (see Figure S1) as a function of pH. The stability and protonation constants of Ga(DATA$^m$) and Ga(DATA$^{5m}$) complexes obtained by pH-potentiometry, $^1$H- and $^{71}$Ga-NMR spectroscopy are listed and compared with those of Ga(AAZTA) in Table 3. The stability constants of Ga(DATA$^m$) and Ga(DATA$^{5m}$) $^-$ complexes are slightly higher than those of Ga(AAZTA)$^-$. Since the total basicity ($\Sigma$log$K^H$) of AAZTA is significantly higher than those of DATA$^m$ and DATA$^{5m}$ (Table 1), the higher log$K_{GaL}$ values of Ga(DATA$^m$) and Ga(DATA$^{5m}$) $^-$ can be explained by considering the structural properties of these complexes. In Ga(DATA$^m$), the Ga$^{3+}$ ion is coordinated by three amine-N and three carboxylate-O donor atoms (two ring- and one exocyclic-carboxylate-O) in a slightly distorted octahedral fashion.[19,20] However, in Ga(AAZTA)$^-$ the Ga$^{3+}$ ion is coordinated by 3 amine-N and 3 carboxylate-O donor atoms (two exocyclic- and one ring-carboxylate-O, whereas one of the ring-carboxylate-O does not coordinate) with a more distorted octahedral geometry , that results in thea less favourable coordination environment for the Ga$^{3+}$-ion and the lower stability

of Ga(AAZTA)$^-$.[12] By taking into account these assumptions and the similar coordination geometry of Ga$^{III}$- and Zn$^{II}$-complexes (both metal ions generally form octahedral complexes), the higher stability of the Zn(DATA$^m$) and Zn(DATA$^{5m}$) by comparing with that of Zn(AAZTA) might also be explained by the less favourable coordination environment of the Zn$^{2+}$-ion in the more distorted Zn(AAZTA) complex. Owing to the higher stability of the Ga(DATA$^m$) and Ga(DATA$^{5m}$), the formation of [Ga(DATA$^m$)OH]$^-$ and [Ga(DATA$^{5m}$)OH]$^{2-}$ (log$K_{GaLH-1}$, Table 3) takes place at higher pH values than that of [Ga(AAZTA)OH]$^{2-}$. However, [Ga(DATA$^m$)OH]$^-$ and [Ga(DATA$^{5m}$)OH]$^{2-}$ species still predominate under physiological conditions (Figures 4 and S3) and are characterized by significantly lower stabilities than that of [Ga(AAZTA)OH]$^{2-}$ (log$\beta_{GaLH-1}$, Table 3), in accord with the different constitution of [Ga(DATA$^m$)OH]$^-$, [Ga(DATA$^{5m}$)OH]$^{2-}$ and [Ga(AAZTA)OH]$^{2-}$.

**Table 1.** Stability and protonation constants of Ga(DATA$^m$), Ga(DATA5$^m$) and Ga(AAZTA) complexes (0.15 M NaCl, 25°C)

| Method | Ga(DATA$^m$) | | Ga(DATA$^{5m}$) | | Ga(AAZTA)[a] |
|---|---|---|---|---|---|
| | pH-pot. | $^1$H/$^{71}$Ga-NMR | pH-pot. | $^1$H/$^{71}$Ga-NMR | pH-pot. |
| | | pH=12 – 1.7 | | | pH=1.7 – 12 |
| log$K_{GaL}$ | 21.54 (2) | 21.80 (4) | 21.41 (2) | 21.60 (5) | 21.15 |
| log$K_{GaHL}$ | 2.42 (2) | 2.25 (9) | 4.44 (3) -COOH | 4.40 (4) -COOH | 3.14 |
| log$K_{GaH2L}$ | – | – | 2.05 (5) | – | 1.14 |
| log$K_{GaLH-1}$ | 6.25 (2) | 6.38 (4) | 6.31 (4) | 6.20 (4) | 4.60 |
| log$\beta_{GaLH-1}$ | 15.29 (2) | 15.42 (4) | 15.07 (4) | 15.40 (5) | 16.57 |

[a] Ref. [12]
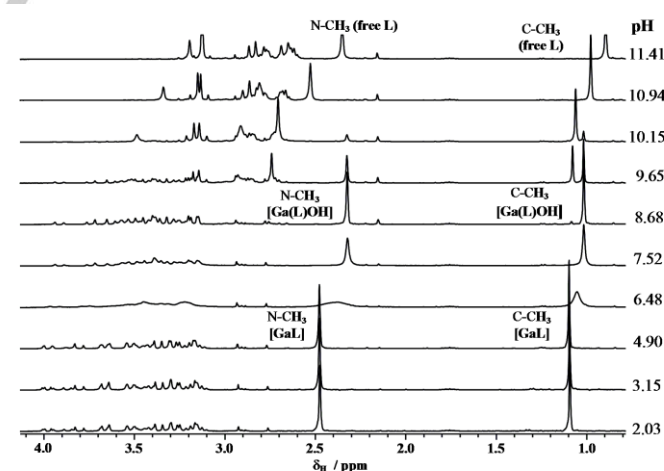


**Figure 2.** 400 MHz $^1$H-NMR spectra of the Ga$^{3+}$ - DATA$^m$ system ([Ga$^{3+}$]=8.15 mM, [DATA$^m$]=8.30 mM, 0.15 M NaCl, 298K)

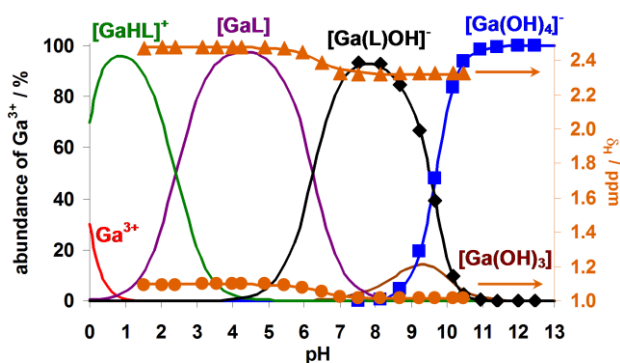The equilibrium data, obtained by pH-potentiometric titration, allowed a calculation of the species distribution diagram for the

Ga$^{3+}$- DATA$^m$ and Ga$^{3+}$- DATA$^{5m}$ systems, (see Figures 4 and S3.)
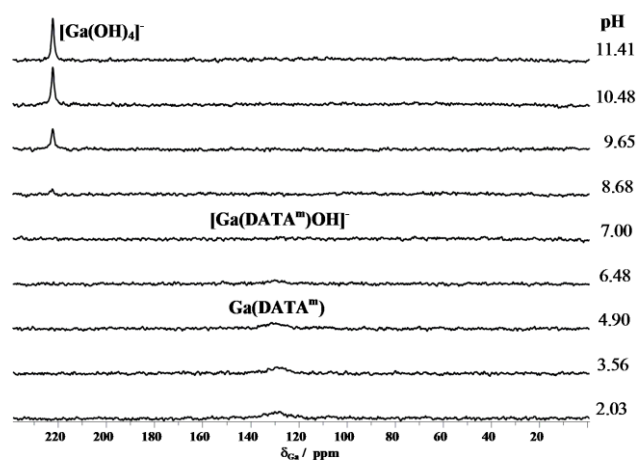


**Figure 3.** 122 MHz $^{71}$Ga-NMR spectra of the Ga$^{3+}$ - DATA$^m$ system ([Ga$^{3+}$]=8.15 mM, [DATA$^m$]=8.30 mM, 0.15 M NaCl, 298K)



**Figure 4.** The species distribution (red, green, purple, black, brown and blue solid lines) in the Ga$^{3+}$ - DATA$^m$ system calculated from pH-potentiometric data (Table 3). ([Ga$^{3+}$] = [**DATA$^m$**] = 8.2 mM, 0.15 M NaCl, 25°C). The percentage of the [Ga(**DATA$^m$**)OH]$^-$ ($\blacklozenge$) and [Ga(OH)$_4$]$^-$ ($\blacksquare$) species were calculated from the $^1$H- and $^{71}$Ga-NMR spectra of the Ga$^{3+}$-**DATA$^m$** system. Chemical shifts of the N-C**H$_3$** ($\blacktriangle$) and C-C**H$_3$** ($\bullet$) protons of Ga(**DATA$^m$)** complex against pH.

In the species distribution diagrams (Figures 4 and S3), the $^1$H- and $^{71}$Ga-NMR data (Figures 2, 3, S1 and S2) indicate that the competition reaction between DATA$^m$ and DATA$^{5m}$ ligands and OH$^-$ ions for the Ga$^{3+}$ ion with the formation of [Ga(DATA$^m$)OH]$^-$ and [Ga(DATA$^{5m}$)OH]$^{2-}$ is complete at about pH<8. In the $^1$H-NMR spectrum, the changes in the intensity and the chemical shifts of the free DATA$^m$ and DATA$^{5m}$ signals indicate the formation of [Ga(DATA$^m$)OH]$^-$ and [Ga(DATA$^{5m}$)OH]$^{2-}$ species and the protonation of free DATA$^m$ and DATA$^{5m}$ ligands in the pH range 8 – 11.4. The $^{71}$Ga-NMR signal is relatively sharp for the highly symmetric [Ga(OH)$_4$]$^-$ species (Figures 3 and S2, $\delta_{Ga}$=223 ppm, $\square_{\frac{1}{2}}$ = 88 Hz) at pH>11. The intensity of the $^{71}$Ga-NMR signal of the [Ga(OH$^-$)$_4$]$^-$ species decreases by decreasing pH due to the formation of [Ga(DATA$^m$)OH]$^-$ and [Ga(DATA$^{5m}$)OH]$^{2-}$ complexes in the pH range 11.4 – 8. In the pH range 7 - 8, the [Ga(DATA$^m$)OH]$^-$ and [Ga(DATA$^{5m}$)OH]$^{2-}$

complexes predominate. At pH<7, the protonation of [Ga(DATA$^m$)OH]$^-$ and [Ga(DATA$^{5m}$)OH]$^{2-}$ complexes by the formation of Ga(DATA$^m$) and Ga(DATA$^{5m}$)$^-$ result in shifts to higher frequency of all the signals in the $^1$H NMR spectrum (Figures 2 and S1). The $^{71}$Ga-NMR signal of the Ga(DATA$^m$) and Ga(DATA$^{5m}$)$^-$ is broad (Figures 3 and S2, Ga(DATA$^m$): $\delta_{Ga}$=129 ppm, $\nu_{\frac{1}{2}}$ = 1000 Hz; Ga(DATA$^{5m}$): $\delta_{Ga}$=129 ppm, $\nu_{\frac{1}{2}}$ = 1100 Hz, pH=4.5). However, the $^{71}$Ga-NMR signal of the Ga(AAZTA)$^-$ is even broader ($\delta_{Ga}$=118 ppm, $\nu_{\frac{1}{2}}$ = 2218 Hz, pH=4.0) as a result of the more asymmetric coordination geometry of AAZTA.[12] In the pH range 3 – 5, the protonation of the n-valeric acid side chain of Ga(DATA$^{5m}$)$^-$ takes place with a shift to higher frequency of the -CH$_2$-COO$^-$ signal (triplet at 2.3 ppm, Figure S1). The protonation constant of n-valeric acid entity of Ga(DATA$^{5m}$)$^-$ (log$K_{GaHL}$=4.40, Table 3) is very similar to that of the free DATA$^{5m}$ (log$K_3^H$=4.35, Table 1), which indicates that the carboxylate group of n-valeric acid arm in DATA$^{5m}$ does not coordinate to the Ga$^{3+}$-ion, so it can protonate/deprotonate independently. In the pH range 1.7 – 3.5, the formation of Ga(HDATA$^m$)$^+$ and Ga(H$_2$DATA$^{5m}$)$^+$ results in a small shift of all signals in the range of 3 – 4 ppm (Figures 2 and S1) which indicates that this process takes place at the weakly-coordinated ring-carboxylate groups of ligands. The stability constant of Ga(DATA$^m$) and Ga(DATA$^{5m}$)$^-$ obtained by the pH-potentiometry and multinuclear NMR spectroscopy) are in very good agreement (see Table 3).

**Dynamic NMR study of chemical exchange processes**

The chemical exchange processes between Ga(DATA$^m$) and [Ga(DATA$^m$)OH]$^-$, and Ga(DATA$^{5m}$)$^-$and [Ga(DATA$^{5m}$)OH]$^{2-}$ complexes have been investigated by $^1$H-NMR spectroscopy in D$_2$O solution (see Figures 5 and S4). The solution structure of Ga(DATA$^{5m}$)$^-$ is expected to be similar to that of the corresponding Ga(DATA$^m$), investigated in the solid state by X-ray diffraction.[19] Crystallographic data of Ga(DATA$^m$) reveal, that the coordination geometry around each Ga$^{3+}$ ion can be described as a slightly distorted octahedral geometry, where one of the ring N, the exocyclic N, one of the ring carboxylate O and the exocyclic carboxylate O donor atoms are coordinated in a square planar fashion in equatorial positions. The other ring N and ring carboxylate O donor atoms complete the coordination sphere of the Ga$^{3+}$-ion in axial positions. [19]

In the $^1$H-NMR spectra (273 K and pH=6.4), signals of the C**H$_3$**-N and C**H$_3$**-C in Ga(DATA$^m$) and the C**H$_3$**-N in Ga(DATA$^{5m}$) give rise to two singlets. By increasing the temperature, the singlets broaden, coalesce (Ga(DATA$^m$): C**H$_3$**-C, T = 283 K; C**H$_3$**-N, T = 298 K; Ga(DATA$^{5m}$): C**H$_3$**-N, T = 298 K) and then merge into a single resonance (Figures 5 and S4). Since at pH=6.4 the Ga(DATA$^m$) and Ga(DATA$^{5m}$)$^-$ complexes are present in the form of GaL and Ga(L)OH species (the ratio of the GaL and Ga(L)OH species is about 2 to 3), this behaviour can be attributed to a chemical exchange process between GaL and Ga(L)OH species via the replacement of one ring carboxylate-O donor atom with an OH$^-$ -ion in the inner sphere of the Ga(DATA$^m$) and Ga(DATA$^{5m}$) complexes (Eq. (8)). Interestingly, the signal of the C**H$_3$**-C protons in the $^1$H-NMR spectra of Ga(AAZTA)$^-$ obtained at 273 K and pH=4.6 (the ratio of GaL and Ga(L)OH species is

about 1 to 1) has not been split to two singlets indicating the differing structures and exchange processes of Ga(AAZTA)⁻ and [Ga(AAZTA)OH]²⁻ complexes (Figure S5).

$$\text{GaL} + \text{OH}^- \rightleftharpoons \text{Ga(L)OH} \qquad (8)$$
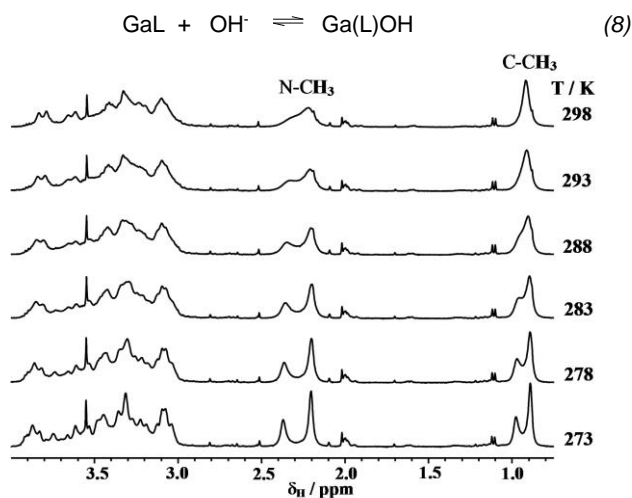


**Figure 5.** VT-400 MHz ¹H-NMR study of Ga(DATAᵐ) – Ga(DATAᵐ)OH system ([GaL]=15 mM, D₂O, pD=6.8 (pD = pH + 0.41))

A complete line-shape analysis allows the extraction of kinetic parameters for the exchange process. The proton NMR spectral data were measured at eight different temperatures, in the range 273-298 K (Figures 5 and S4). The limiting value of the transverse relaxation time ($T_2$) has been calculated from the line width of the singlet at 3.55 ppm (Figure 5) ($T_2 = 0.07$ s), because of its temperature independence below 298 K. The chemical shift differences ($\Delta\delta$, between the C**H₃**-C and C**H₃**-N protons of Ga(DATAᵐ) and [Ga(DATAᵐ)OH]⁻ complexes are 35 and 67 Hz, whereas the $\Delta\delta$ value for the C**H₃**-N protons in Ga(DATA⁵ᵐ)⁻ and [Ga(DATA⁵ᵐ)OH]²⁻ complexes is 66 Hz.
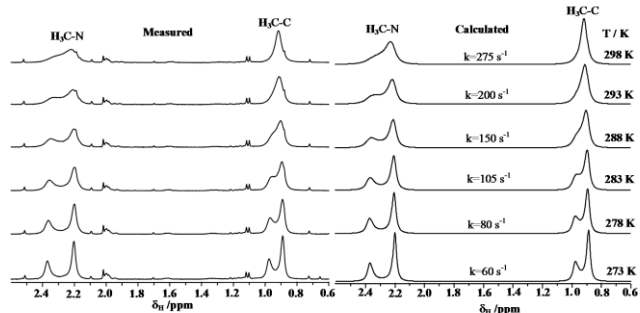


**Figure 6.** Experimental and calculated ¹H-NMR spectra (400 MHz) of the N-CH₃ and C-CH₃ protons in Ga(DATAᵐ) – Ga(DATAᵐ)OH systems as a function of temperature.

The activation parameters were assessed from the temperature dependence of the calculated rate constants ($k_{ex}=1/\tau$) using the *Eyring* equation (Figure S7). The activation parameters for the

exchange reaction between GaL and Ga(L)OH species of Ga(DATAᵐ) and Ga(DATA⁵ᵐ) complexes are listed in Table 4.

**Table 4.** Rate constant and activation parameters for the exchange reaction between GaL and Ga(L)OH species of Ga(DATAᵐ) and Ga(DATA⁵ᵐ) complexes obtained from the line-shape analysis of the ¹H-NMR spectra.

|  | Ga(DATAᵐ) | Ga(DATA⁵ᵐ) |
|---|---|---|
| $\Delta H^{\#}$ /kJ·mol⁻¹ | 39 (1) | 32.7 (8) |
| $\Delta S^{\ddagger}$ /J·mol⁻¹K⁻¹ | -67 (4) | -89 (3) |
| $\Delta G^{\ddagger}_{298}$ /kJ·mol⁻¹ | 59.0 (1) | 59.3 (1) |
| $k^{298}$ /s⁻¹ | 280 | 250 |

The band shape analysis provides very similar free energy ($\Delta G^{\ddagger}_{298}$), activation enthalpy ($\Delta H^{\#}$) and activation entropy ($\Delta S^{\ddagger}$) values for the exchange reactions between GaL and Ga(L)OH species for the Ga(DATAᵐ) and Ga(DATA⁵ᵐ) complexes. In fact, the same exchange processes for Ga(DATAᵐ) and Ga(DATA⁵ᵐ) complexes take place with similar activation parameters, which is clearly indicated by the similar exchange rates ($k_{ex}^{298}$) (Table 4), and the similar slopes and the intercepts obtained from the *Eyring* plots (Figure S7). The formation of Ga(L)OH species from both Ga(DATAᵐ) and Ga(DATA⁵ᵐ) complexes requires the decoordination of a ring carboxylate O donor atom and the coordination of OH⁻ ion. It results in the weakening of the bonds formed between the Ga³⁺-ion and the nitrogen donor atoms of the ring. Since the exchange between GaL and Ga(L)OH species for Ga(AAZTA)⁻ takes place more rapidly even at low temperature, (Figure S5) it can be assumed that the formation of Ga(L)OH species occurs by the (relatively slow) structural rearrangement of the Ga(DATAᵐ) and Ga(DATA⁵ᵐ) complexes, as characterized by relatively high $\Delta G^{\ddagger}_{298}$ values.

**Dissociation kinetics**

In order to apply the Ga(DATAᵐ) and Ga(DATA⁵ᵐ) complexes as ⁶⁸Ga based radiodiagnostics *in vivo*, their kinetic stability with respect to metal dissociation must be evaluated. Nowadays, it is generally accepted that the kinetic inertness of metal complexes in vivo is more important then the thermodynamic stability, especially for shorter-lived radioisotope complexes. The inertness can avoid a rapid loss of the metal ion and the loss of radioactivity from the targeted agent. The dissociation rate of the metal ion from a Gaᴵᴵᴵ-complex is typically measured in strong acidic ([H⁺]>1.0 M) and/or strong basic conditions ([OH⁻]>0.1 M).[8a,27] These conditions differ considerably from the physiological ones and limiting the value of the data to predict the behaviour of metal complexes in body fluids for *in vivo* experiments. The intravenously administered Gaᴵᴵᴵ-complex may interact with the endogenous ions (Cu²⁺, Zn²⁺ and Ca²⁺) or serum proteins such as transferrin, that results in the release of the Ga³⁺ ion. In order to assess the kinetic inertness, the trans-metallation and trans-chelation reactions of Ga(DATAᵐ) and Ga(DATA⁵ᵐ) complexes with Cu²⁺ and transferrin have been studied by spectrophotometry.

*Transmetallation reactions*: The transmetallation reactions occurring between the Ga$^{III}$ chelates and Cu$^{2+}$ ions have been studied by spectrophotometry examining the absorption band of the resulting Cu$^{II}$-complexes in the presence of excess citrate, to prevent the hydrolysis of Ga$^{3+}$ and Cu$^{2+}$ ions over the pH range 6.0 – 9.0. Under such conditions Cu$^{2+}$ is predominantly present as Cu(Cit)H$_{-1}$ species, whereas the Ga$^{3+}$ ion forms Ga(Cit)H$_{-1}$ and Ga(Cit)$_2$ complexes.[12,28] The absorption spectra of the Ga(DATA$^m$)$^-$ and Cu$^{2+}$-citrate as well as the Ga(DATA$^{5m}$)$^-$ and Cu$^{2+}$-citrate reacting systems are presented in Figures 7 and S8. The trans-metallation reactions can be described as follows:

$$GaL + Cu^{2+} \rightleftharpoons CuL + Ga^{3+} \qquad (9)$$
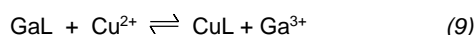
The rates of the trans-metallation reactions have been studied in the presence of excess of GaL complexes ([GaL]$_{tot}$/[Cu$^{2+}$]$_{tot}$ = 10 and 20) when a pseudo-first order kinetic model can be applied and the rates of reaction can be expressed by Eq. (10):

$$-\frac{d[GaL]_t}{dt} = \frac{d[CuL]_t}{dt} = k_d[GaL]_t \qquad (10)$$

where $k_d$ is a pseudo-first-order rate constant, [GaL]$_t$ and [CuL]$_t$ are the total concentration of complexes (e.g. GaL, Ga(L)OH, CuL) at the time $t$, respectively. During the course of transmetallation reactions, the concentration of Cu(DATA$^m$) and Cu(DATA$^{5m}$) complexes increase, while that of Cu(Cit)H$_{-1}$ decreases.
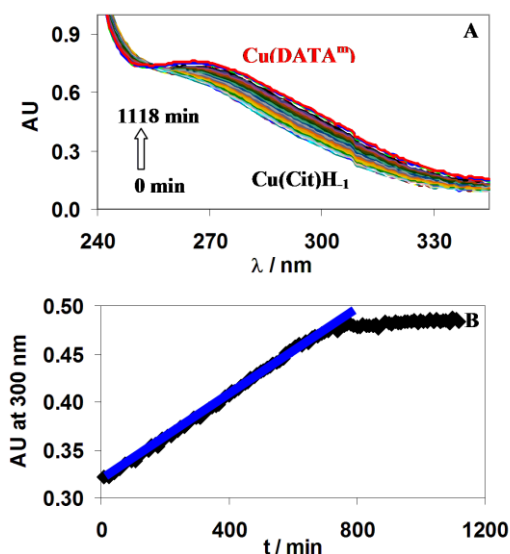


**Figure 7.** Absorption spectra (**A**) and absorbance values measured at 300 nm (**B**) for the Ga(DATA$^m$) – Cu$^{2+}$ reacting system in the presence of citrate. The blue line represents the slope of the kinetic curve ($\Delta$Abs/$\Delta$t) used for the calculation of $k_d$ values. ([GaL]=2.0 mM, [Cu$^{2+}$]=0.2 mM, [Cit]=2.0 mM, [MES]=0.01 M, pH=6.0, 0.15 M NaCl, 298 K, l=1 cm).

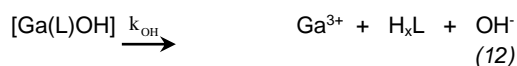By the use of 1.0 cm cells, the first-order rate constant, $k_d$ can be calculated by Eq. (11):

$$k_d = \frac{\Delta Abs}{\Delta t} \times \frac{1}{\varepsilon_{CuL} - \varepsilon_{Cu(Cit)H_{-1}}} \times \frac{1}{[GaL]_t} \qquad (11)$$

In Eq. (11) $\Delta$Abs/$\Delta$t values (the increase of the absorbance during the time $\Delta$t) are calculated from the slope of the kinetic curves. $\varepsilon_{Cu(Cit)H-1}$ and $\varepsilon_{CuL}$ are the molar absorptivities of the Cu(Cit)H$_{-1}$ (921 M$^{-1}$cm$^{-1}$), Cu(DATA$^m$) (1406 M$^{-1}$cm$^{-1}$) and Cu(DATA$^{5m}$) (2146 M$^{-1}$cm$^{-1}$) complexes at 300 nm. (The absorption of Ga$^{3+}$ containing species at 300 nm can be neglected.) The pseudo-first-order rate constants obtained for the reactions of Ga(DATA$^m$) and Ga(DATA$^{5m}$) with Cu$^{2+}$ at different pH values in the presence of citrate are shown in Figure 8.
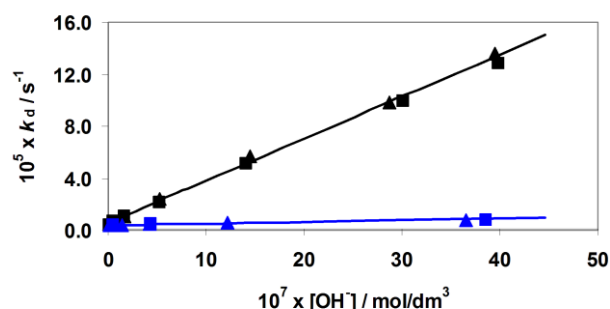


**Figure 8.** $k_d$ values vs. [OH$^-$] for the reaction of **Ga(DATA$^m$)** and **Ga(DATA$^{5m}$)** with Cu$^{2+}$. ([Ga(DATA$^m$)] = [Ga(DATA$^{5m}$)]=2.0 mM, [Cu$^{2+}$]=0.1 (■, ■) and 0.2 mM (▲, ▲) [Cit]=2.0 mM, [MES]=[HEPES] = 0.01 M, 0.15 M NaCl, 25°C).

The $k_d$ values presented in Figure 8 are independent of the concentration of Cu$^{2+}$ and Cu(Cit)H$_{-1}$, indicating that the rate determining step of the exchange reactions is the dissociation of the Ga$^{III}$-complexes. Since the rate data have been obtained in the pH range 6-8.5, and according to the species distribution plots (Figures 4 and S3) at pH=6 approximately 40% of the Ga$^{3+}$ is present in the form of (GaL)OH and with increasing pH the concentration of these species increases and at pH=7.5 it is about 90 %, it can be assumed that the dissociable complex is the Ga(L)OH. (In the ternary Ga(L)OH complexes the DATA$^m$ and DATA$^{5m}$ ligands are coordinated by 5 donor atoms only and the electrostatic repulsion between the donor atoms and the OH$^-$ ion is also stronger than in the GaL parent complexes. Therefore, the spontaneous dissociation of the Ga(L)OH species is more probable.) Since the $k_d$ values (see Figure 8) are directly proportional to the OH$^-$ concentration and the straight line shows a non-zero intercept, we assume that the dissociation of Ga(L)OH complexes may occur spontaneously and with the assistance of OH$^-$ ions, as indicated by Equations (12) and (13):

$$[Ga(L)OH] \xrightarrow{k_{OH}} Ga^{3+} + H_xL + OH^- \qquad (12)$$

$$[Ga(L)OH] + OH^- \xrightarrow{k_{OH^2}} Ga^{3+} + H_xL + 2OH^- \qquad (13)$$

The rate determining dissociation of complexes is followed by the rapid reaction of free ligands with the Cu$^{2+}$ ions. By taking into account the two pathways, the rate of the dissociation of Ga(DATA$^m$) and Ga(DATA$^{5m}$) can be expressed by Eq. (14).

*(14)*Considering the total concentration of the complex ([GaL]$_{tot}$ = [GaL]+[Ga(L)OH]) and the protonation constant of Ga(L)OH species ($K_{GaLH-1}$, Eq. (4)), the pseudo-first-order rate constants ($k_d$, (Eq. 10)) can be expressed as follows:

$$k_d = \frac{(k_{OH}[OH^-] + k_{OH^2}[OH^-]^2)(K_w K_{GaLH-1})^{-1}}{1 + [OH^-](K_w K_{GaLH-1})^{-1}} \qquad (15)$$

where $K_W$ is the ionic product of water (p$K_w$=13.85, 0.15 M NaCl, 25°C), whereas $k_{OH}$ and $k_{OH}^2$ rate constants characterizing the spontaneous and OH⁻ assisted dissociation of Ga(DATA$^m$)OH and Ga(DATA$^{5m}$)OH, respectively. The rate and equilibrium constants characterising the transmetallation reaction of Ga(DATA$^m$) and Ga(DATA$^{5m}$) were calculated by fitting the $k_d$ values presented in Figure 8 to the Eq. (15) and the values obtained are shown and compared with those of Ga(AAZTA)⁻ in Table 5. The "deprotonation" constants (log$K_{GaLH-1}$) obtained by pH-potentiometry (Table 3) and from kinetic data are in good agreement.

**Table 5.** Rate and equilibrium constants and half-lives ($t_{1/2}$=ln2/$k_d$) for the transmetallation reactions of Ga(DATA$^m$), Ga(DATA$^{5m}$) and Ga(AAZTA) complexes (0.15 M NaCl, 25°C)

| | Ga(DATA$^m$) | Ga(DATA$^{5m}$) | Ga(AAZTA) [a] |
|---|---|---|---|
| $k_{OH}$ / s$^{-1}$ | $(8.0 \pm 0.2) \times 10^{-6}$ | $(4.2 \pm 0.1) \times 10^{-6}$ | $3.0 \times 10^{-6}$ |
| $k_{OH^2}$ / M$^{-1}$s$^{-1}$ | $31 \pm 1$ | $1.2 \pm 0.1$ | 10 |
| $K_{GaLH-1}$ | $(1.6 \pm 0.1) \times 10^6$ | $(1.7 \pm 0.2) \times 10^6$ | $1.4 \times 10^9$ |
| p$K_w$[b] | 13.85 | | |
| log$K_{GaLH-1}$ | 6.20 (2) | 6.25 (4) | 4.72 |
| $k_d$ / s$^{-1}$ (pH=7.4) | $1.7 \times 10^{-5}$ | $4.3 \times 10^{-6}$ | $9.2 \times 10^{-6}$ |
| $t_{1/2}$ / h (pH=7.4) | 11 | 44 | 21 |

[a] Ref. [12], [b] Ionic product of water determined by pH-potentiometry (0.15 M NaCl, 25°C)

The $k_{OH}$ and the $k_{OH}^2$ rate constants characterizing the spontaneous and OH⁻ assisted dissociation of Ga(DATA$^m$)OH are somewhat higher than the corresponding rate constants of Ga(AAZTA)OH. Interestingly, the $k_{OH}^2$ rate constant characterizing the OH⁻ assisted dissociation of Ga(DATA$^{5m}$)OH is about 8 times lower than the corresponding rate constant of Ga(AAZTA)OH. The spontaneous dissociation of Ga(DATA$^m$)OH, Ga(DATA$^{5m}$)OH and Ga(AAZTA)OH likely proceeds through the intramolecular rearrangement of the Ga$^{III}$ complexes that results in a cascade-like de-coordination of each donor atom, with the consequent release of the Ga$^{3+}$ ion. The more rapid spontaneous dissociation of Ga(DATA$^m$)OH and Ga(DATA$^{5m}$)OH can be interpreted in terms of the distorted coordination around the Ga$^{3+}$-ion, that causes the faster intramolecular rearrangement of the Ga(L)OH species. With the use of the rate and equilibrium constants presented in Table 5, the half-lives ($t_{1/2}$=ln2/$k_d$) of the dissociation reactions of

Ga(DATA$^m$) and Ga(DATA$^{5m}$) at pH=7.4 have been calculated and compared with that of Ga(AAZTA). The $t_{1/2}$ values of Ga(DATA$^m$), Ga(DATA$^{5m}$) and Ga(AAZTA)⁻ are 11, 44 and 21 hours, respectively, consistent with the higher kinetic inertness of Ga(DATA$^{5m}$) due to the slower OH⁻ assisted dissociation of the [Ga(DATA$^{5m}$)OH] species.

*Exchange reactions with transferrin.* Because of the relatively high concentration of transferrin in human plasma[28] and the strong affinity of Ga$^{3+}$ to transferrin (Ga$^{3+}$-transferrin: log$K_{GaTf}$=18.9, log$K_{Ga2Tf}$=17.7)[29] this protein may compete with DATA$^m$ and DATA$^{5m}$ for the Ga$^{3+}$ ion leading to the dissociation of Ga(DATA$^m$) and Ga(DATA$^{5m}$). In order to determine the extent of trans-chelation between Ga(DATA$^m$), Ga(DATA$^{5m}$) and transferrin, the ligand exchange reactions between Ga$^{III}$-complexes and human serum transferrin (sTr) were studied by spectrophotometry at the absorption band of the Ga$^{3+}$-sTf complex in the 240 - 250 nm range (Figures 9 and S9). The absorbance values of the Ga(DATA$^m$) - sTf and Ga(DATA$^{5m}$) - sTf reacting systems obtained at [GaL]= 0.2 and 0.3 mM are shown in Figures S10 and S11. The ligand exchange reaction between Ga(DATA$^m$), Ga(DATA$^{5m}$) and human sTf is expressed by Eq. (17):

$$Ga(L) + sTf \rightleftharpoons Ga(sTf) + L \qquad (16)$$
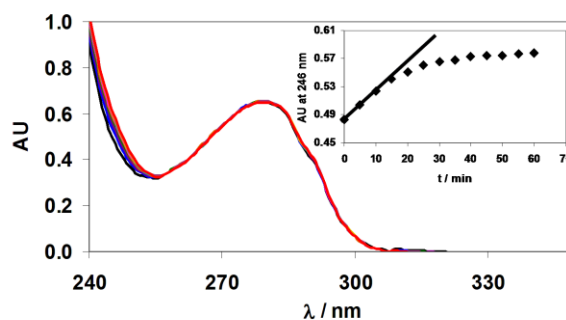
**Figure 9.** Absorption spectra of the Ga(DATA$^m$) - transferrin system. Inserted figure shows the absorbance values of the reacting system at 246 nm as a function of time ([GaL] = 0.2 mM, [Trf] = 10 μM, [NaHCO$_3$]=25 mM, pH = 7.4, 0.15 M NaCl, 25°C).

The rates of the ligand exchange reaction were studied in the presence of high excess of Ga(DATA$^m$) and Ga(DATA$^{5m}$) ([GaL]=0.2 and 0.3 mM, [sTf]= 10 μM). Under such conditions, the ligand exchange reaction can be treated as a pseudo-first-order process and the rate of the reaction can be expressed by Equation (10). By taking into account the molar absorptivity of Ga(sTf) ($\varepsilon_{246}$=13800 cm$^{-1}$M$^{-1}$),[12] the rate constants ($k_d$) were calculated from the slope of the kinetic curves ($\Delta$Abs/$\Delta$t, Figures S10 and S11) with Equation (11) (the middle term in Equation (11) has been replaced by $1/\varepsilon_{Ga(sTf)}$). The slope of the kinetic curves were considered up to 30 % conversion, in order to be sure of the Ga(sTf) complex formation. The rate constant ($k_d$) and half-life ($t_{1/2}$=ln2/$k_d$) values obtained for the transchelation reactions are shown and compared with that of Ga(AAZTA) in Table 6. The $k_d$ rate constants obtained for the ligand exchange reaction of Ga(DATA$^m$) and Ga(DATA$^{5m}$) with sTf (Table 6) and

the metal exchange reactions of Ga(DATA$^m$) and Ga(DATA$^{5m}$)with Cu$^{2+}$ in the presence of citrate (Table 5) are essentially equal. These findings suggest that human transferrin has no effect on the rate of dissociation, which practically takes place through the spontaneous and hydroxide assisted dissociation of GaL and Ga(L)OH species followed by the fast reaction between the released Ga$^{3+}$ ion and human sTf. The dissociation half-life values of Ga(DATA$^m$) calculated from the trans-metallation studies ($t_{1/2}$=11 h) and from the ligand exchange reactions ($t_{1/2}$=9.4 h) indicates that the kinetic inertness of Ga(DATA$^m$) is lower than that of Ga(AAZTA). However, the dissociation half-life of Ga(DATA$^{5m}$) is about four and two times higher than that of Ga(DATA$^m$) and Ga(AAZTA), respectively.

**Table 6.** Rate constants ($k_d$) and half-lifes ($t_{1/2}$=ln2/$k_d$) characterizing the trans-chelation reactions of Ga(DATA$^m$), Ga(DATA$^{5m}$) and Ga(AAZTA) complexes with transferrin (0.15 M NaCl, 25°C, pH=7.4)

|  | Ga(DATA$^m$) | Ga(DATA$^{5m}$) | Ga(AAZTA)[a] |
|---|---|---|---|
| $k_d$ / s$^{-1}$ | (21±0.1)×10$^{-6}$ | (4.2±0.2)×10$^{-6}$ | 8.0×10$^{-6}$ |
| $t_{1/2}$ / h | 9.4 | 46 | 24 |

[a] Ref. [12]

On the basis of these results ligands based on Ga(DATA$^{5m}$) represent good candidates for the development of the Ga$^{3+}$-based radiodiagnostics, in accord with the excellent PET images obtained in recent $^{68}$Ga radiolabelling experiments on peptide conjugates. [21]

## Conclusions

The complexation properties of the AAZTA derivative hexadentate DATA$^m$ and DATA$^{5m}$ ligands have been studied by by pH-potentiometry, spectrophotometry and $^1$H- and $^{71}$Ga-NMR spectroscopy. The complex forming ability of the new derivatives with Ga$^{3+}$ and Zn$^{2+}$ is higher than that of heptadentate AAZTA, while the stabilities of Ca$^{2+}$, Mn$^{2+}$ and Cu(AAZTA) complexes are higher than those of the DATA$^m$ and DATA$^{5m}$ ligands. Owing to the strong affinity of OH$^-$ ions to Ga$^{3+}$, at physiological pH the mono-hydroxo Ga(L)OH complexes predominate.

The rates of exchange reaction between the Ga(L) and Ga(L)OH complexes were studied by $^1$H-NMR spectroscopy in the temperature range 273-293 K. The trans-metallation reactions between the Ga(DATA$^m$) and Ga(DATA$^{5m}$) complexes and Cu$^{2+}$-citrate and the ligand exchange reactions between the Ga$^{III}$-complexes and the serum protein transferrin in the pH range of 6-8.5 occur through the same mechanism. The metal and ligand exchange reactions take place through the spontaneous and OH$^-$ assisted dissociation of the Ga(L)OH complexes. The half lives of the dissociation of Ga(DATA$^m$), Ga(DATA$^{5m}$) and Ga(AAZTA) are 11 h, 44 h and 24 h, respectively. Based on the equilibrium and kinetic properties the $^{68}$Ga(DATA$^{5m}$) complex and its derivatives constitute a promising family of candidates as radiopharmaceutical agents for the use in PET diagnostics.

## Experimental Section

### 1. General

New compounds were characterized by $^1$H, $^{13}$C, $^1$H-$^1$H-COSY, HSQC, HMBC, MS, and HRMS. $^1$H (400 MHz) and $^{13}$C NMR (100 MHz) spectra were obtained with with Bruker Avance III HD 400 (9.4 T) by the use of TMS as internal standard. Column chromatography was performed on silica gel (MERCK silica gel 60). Purification via HPLC was performed on a column from Phenomenex (Luna 10 u (C18) 100 A (250x10.00 mm 10 micron)). As mobile phase a system of water (0.1 %TFA; A) and acetonitrile (0.1 % TFA; B) was used.

### 2. Materials

Ga(NO$_3$)$_3$ was prepared by dissolving Ga$_2$O$_3$ (99.9%, Fluka) in 6M HNO$_3$ and evaporating of the excess acid. The solid Ga(NO$_3$)$_3$ was dissolved in 0.1 M HNO$_3$ solution. The concentration of the Ga(NO$_3$)$_3$ solution was determined by using the standardized Na$_2$H$_2$EDTA in excess. The excess of the Na$_2$H$_2$EDTA was measured with standardized ZnCl$_2$ solution and xylenol orange as indicator. The concentration CaCl$_2$ (Sigma), MnCl$_2$ (Sigma), ZnCl$_2$ (Sigma) and CuCl$_2$ (Sigma) solutions were determined by complexometric titration with standardized Na$_2$H$_2$EDTA and xylenol orange (ZnCl$_2$), murexide (CuCl$_2$) *Patton & Reeder* (CaCl$_2$) and eriochrome black T (MnCl$_2$) as indicator. The H$^+$ concentration of the Ga(NO$_3$)$_3$ solution was determined by pH potentiometric titration in the presence of excess Na$_2$H$_2$EDTA. The concentration of H$_3$DATA$^m$, H$_4$DATA$^{5m}$ and H$_4$AAZTA (provided by Prof. Giovanni Battista Giovenzana, Dipartimento di Scienze del Farmaco, Università del Piemonte Orientale, Novara, Italy) stock solutions was determined by pH-potentiometric titrations in the presence and absence of a 40-fold excess of Ca$^{2+}$. The citrate solution was prepared from H$_3$Citrate (Sigma) and its concentration was determined by pH-potentiometry. The pH-potentiometric titrations were made with standardized 0.2 M NaOH.

### 3. Synthesis of DATA$^m$:

*N,N'-Dibenzyl-N,N'-di-(tert-butylacetate)-ethylendiamine (1)*: N,N'-dibenzylethylenediamine (3.00 g; 12.48 mmol) and Na$_2$CO$_3$ (5.12 g; 48.67 mmol) were stirred at room temperature in dry acetonitrile (50 mL) for 30 min. *Tert*-butylbromoacetate (4.64 g; 23.72 mmol), dissolved in dry acetonitrile (10 mL), was added at room temperature over period of 30 min. After completion the suspension was heated over night at 90 °C, filtrated and the filtrate was concentrated under vacuum. After purification via column chromatography (H/EA; 6:1; 0.25) the product was obtained as colourless solid (5.56 g; 11.9 mmol; 95 %).
$^1$H-NMR (CDCl$_3$, 400 MHz): 7.34-7.21 (m, 10 H); 3.78 (s, 4 H); 3.26 (s, 4H); 2.82 (s, 4 H); 1.44 (s, 18 H); $^{13}$C-NMR (CDCl$_3$, 100 MHz): 171.03 (s); 139,18 (s); 129.05 (s); 128.30 (s); 127.10 (s); 80.86 (s); 58.39 (s); 55.27 (s); 51.73 (s); 28.24 (s) MS (ESI$^+$): 469.28, 470.31, 471.33 (M+H$^+$)

*1,4-Di(tert-butylacetate)-6-methyl-6-nitroperhydro-1,4-diazepane (2)*: 1 (0.29 g; 0.92 mmol) was dissolved in 5 mL abs. ethanol and formic acid (69 µL; 1.84 mmol). To this solution Pd/C (0.06 g; 16 wt%) was added and the solution was saturated and kept overnight with hydrogen. After completion the Pd/C was filtrated over celite, the filtrate was concentrated and dried. The crude product 2a (0.29 g; 0.89 mmol; 96 %) was used without further purification. Nitroethane (89 µL; 1.25 mmol) and 2a (0.29 g; 0.89 mmol) was dissolved in dry methanol (5 mL) and heated overnight. The solution was concentrated under vacuum and purified via column chromatography (H/EA, 5:1; R$_f$ =0.24 ). The product was obtained as yellowish oil (0.18 g; 0.46mmol; 52 %).

^{1}H-NMR (CDCl3, 400 MHz): 3.66 (d, J = 14.9 Hz, 2 H); 3.49 (d, J = 17.5 Hz, 2 H); 3.38 (d, J = 17.5 Hz, 2 H); 3.13 (d, J = 14.9 Hz, 2 H); 2.89 (m, 4 H); 1.46 (s, 21 H); ^{13}C-NMR (CDCl3, 100 MHz): 170.83 (s); 91.80 (s); 81.42 (s); 77.48 (s); 77.16 (s); 76.84 (s); 62.38 (s); 60.85 (s); 56.52 (s); 28.36 (s); 24.07 (s) MS (ESI[+]): 388.14, 389.18, 390.20 (M+H^{+})

*1,4-Di(tert-butylacetate)-6-methyl-6-(amino-tert-butylacetate)-perhydro-1,4-diazepane (3)*: **2** (0.16 g; 0.41 mmol) was dissolved in absolute ethanol (2.5 mL), combined with RaneyNickel 2800® (0.1 g) (washed 4 times with ethanol) and the suspension was saturated with hydrogen and stirred at 40 °C for 6 h. After completion the RaneyNickel was filtrated over Celite/sand, the filtrate was concentrated and dried under vacuum. The product **3a** (0.09 g; 0.28 mmol) was dissolved with diisopropylethylamine (49 µL; 0.28 mmol) in dry acetonitrile and stirred under nitrogen for 30 minutes at room temperature. *Tert*-butylbromoacetate (0.05 g; 0.25 mmol) was added dropwise to the solution and stirred at room temperature overnight. The solution was concentrated under vacuum and purified via column chromatorgraphy (H/EA, 2:1; Rf = 0.39). The product **3** was obtained as yellow oil (0.06 g; 0.13 mmol; 45 %).
^{1}H-NMR (CDCl3, 400 MHz): 3.30 (s, 2 H); 3.26 (s, 2 H); 2.79 (m, 4 H); 2.67 (m, 4 H); 1.45 (s, 9 H); 1.43 (s, 18 H) 0.92 (s, 3 H) ; ^{13}C-NMR (CDCl3, 100 MHz): 171.94 (s); 80.95 (s); 64.72 (s); 61.95 (s); 57.29 (s); 56.02 (s); 45.08 (s); 28.34 (s); 28.26 (s); 22.76 (s) MS (ESI[+]): 472.31, 473.13, 474.35 (M+H^{+}).

*1,4-Di(tert-butylacetate)-6-methyl-6-(amino(methyl)-tert-butylacetate)-perhydro-1,4-diazepane (4)*: **3** (0.21 g, 0.46 mmol) was dissolved in acetonitrile (5 mL), formalin solution (379 µL, 4.56 mmol, 37 wt%) and acetic acid (77 µL, 1.35 mmol) and stirred for 30 min at room temperature. To this solution sodium borohydride (0.05 g, 1.35 mmol) was added portion wise and stirred for 1 h at room temperature. After completion the mixture was quenched with water (10 mL), extracted with chloroform and concentrated under vacuum. The residue was purified via column chromatography (H/EA, 1:1; Rf = 0.12). The product **4** was obtained as yellowish oil (0.16 g, 0.32 mmol; 70 %).
^{1}H-NMR (CDCl3, 400 MHz): 3.44 (s, 2 H); 3.27 (s, 4 H); 2.94 (d, 2 H, J = 14.1 Hz); 2.82-2.67 (m, 4 H); 2.57 (d, 2 H, J = 14.1 Hz); 2.32 (s, 3 H); 1.45 (s, 27 H); 1.08 (s, 3 H); ^{13}C-NMR (CDCl3, 100 MHz): 172.00 (s); 171.03 (s); 80.97 (s); 80.58 (s); 63.41 (s); 62.45 (s); 61.02 (s); 59.06 (s); 54.42 (s); 37.47 (s); 28.36 (s); 28.28 (s); 23.79 (s) MS (ESI[+]): 486.30, 487.33, 488.37 (M+H^{+})

*1,4-Di(acetate)-6-methyl-6-(amino(methyl)-acetate)-perhydro-1,4-diazepane (5)*: **4** (0.12 g; 0.25 mmol) was dissolved in dichlormethane (2 mL) and trifluoracetic acid (0.7 mL) and stirred for 19 h at room temperature. After completion of the reaction the solution was concentrated under vacuum. The residue was dissolved in acetonitrile (1 mL), ice cold diethylether was added and the product was precipitated as colourless solid (23.8 mg; 0.08 mmol; 30 %; tR = 7.0 min (0 % to 30 % **B** in 20 min)). ^{1}H-NMR (CDCl3, 400 MHz): 3.45 (s, 2 H); 3.27 (s, 4 H); 2.94 (d, 2 H, J = 14.1 Hz); 2.78 (m, 2 H); 2.57 (d, 2 H, J = 14.1 Hz); 2.33 (s, 3 H), 1.45 (s, 27 H); 1.08 (s, 3 H); ^{13}C-NMR (CDCl3, 100 MHz): 174.42 (s); 170.27 (s); 59.87 (s); 55.81 (s); 55.14 (s); 54.65 (s); 43.77 (s); 37.39 (s); 13.15 (s) HR-MS (ESI[+]): 340.1476, 341.1537, 342.1546 (M+H^{+})
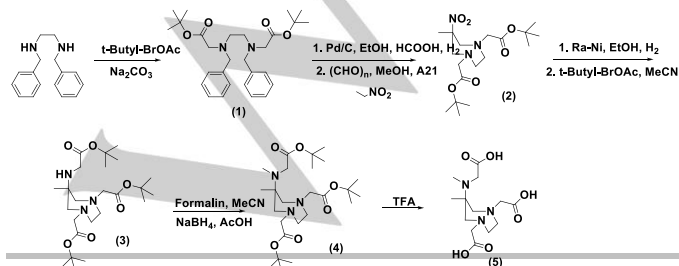


## 4. Synthesis of DATA[5m]

*N,N'-Dibenzyl-N,N'-di-(tert-butylacetate)-ethylendiamine (1)*: N,N´-dibenzylethylenediamine (3.00 g; 12.48 mmol) and Na2CO3 (5.12 g; 48.67 mmol) were stirred at room temperature in dry acetonitrile (50 mL) for 30 min. *Tert*-butylbromoacetate (4.64 g; 23.72 mmol), dissolved in dry acetonitrile (10 mL), was added at room temperature over period of 30 min. After completion the suspension was heated over night at 90 °C, filtrated and the filtrate was concentrated under vacuum. After purification via column chromatography (H/EA; 6:1; Rf = 0.25) the product was obtained as colourless solid (5.56 g; 11.87 mmol; 95 %).
^{1}H-NMR (CDCl3, 400 MHz): 7.34-7.21 (m, 10 H); 3.78 (s, 4 H); 3.26 (s, 4H); 2.82 (s, 4 H); 1.44 (s, 18 H); ^{13}C-NMR (CDCl3, 100 MHz): 171.03 (s); 139,18 (s); 129.05 (s); 128.30 (s); 127.10 (s); 80.86 (s); 58.39 (s); 55.27 (s); 51.73 (s); 28.24 (s) MS (ESI[+]): 469.28, 470.31, 471.33 (M+H^{+})

*1,4-Di(tert-butylacetate)-6-methylpentonate-6-nitroperhydro-1,4-diazepane (2)*: **1** (3.89 g; 8.32 mmol) was dissolved in 20 mL abs. ethanol and formic acid (627.8 µL; 16.64 mmol). To this solution Pd/C (0.62 g; 16 wt%) was added and the solution was saturated and kept overnight with hydrogen. After completion the Pd/C was filtrated over celite, the filtrate was concentrated and dried. The crude product **2a** (2.29 g; 8.12 mmol; 98 %) was used without further purification. A solution of 2-nitrocyclohexanone (1.16 g; 8.12 mmol) and amberylst A21 (2 mass-eq) in dry methanol (30 mL) was heated for 1 h. Then product **2a** (2.29 g; 8.12 mmol) and paraformaldehyde (0.88 g; 29.23 mmol) was added and the suspension was heated overnight under reflux. The suspension was filterated, the filtrate was concentrated under vacuum and purified via column chromatography (H/EA, 2:1; Rf = 0.43). The product **2** was obtained as yellowish oil (2.66 g; 5.50 mmol; 67 %).
^{1}H-NMR (CDCl3, 400 MHz): 3.65 (s, 3 H); 3.60 (d, J = 14.6 Hz, 2 H); 3.45 (d, J = 17.3 Hz, 2 H); 3.30 (d, J = 17.3 Hz, 2 H); 3.12 (d, J = 14.6 Hz, 2 H); 2.84 (m, 4 H); 2.27 (t, 3 H); 1.83 (m, 2 H), 1.57 (m, 2 H); 1.46 (s, 18 H); 1.18 (m, 2 H); ^{13}C-NMR (CDCl3, 100 MHz): 173.73 (s); 170.92 (s); 95.12 (s); 81.31 (s); 61.57 (s); 61.18 (s); 56.87 (s); 51.68 (s); 37.27 (s); 33.71 (s); 28.35 (s); 24.82 (s); 22.99 (s) MS (ESI[+]): 488.27, 489.29, 490.31 (M+H^{+})

*1,4-Di(tert-butylacetate)-6-methylpentonate-6-amino-tert-butylacetate-perhydro-1,4-diazepane (3)*: **2** (1.59 g; 3.27 mmol) was dissolved in absolute ethanol (15 mL), combined with RaneyNickel 2800® (0.5 g) (washed 4 times with ethanol) and the suspension was saturated with hydrogen and stirred at 40 °C for 6 h. After completion the RaneyNickel was filtrated over Celite/sand, the filtrate was concentrated and dried under vacuum. The product **3a** (1.08 g; 2.36 mmol) was dissolved with diisopropylethylamine (419 µL; 2.36 mmol) in dry acetonitrile and stirred under nitrogen for 30 minutes at room temperature. *Tert*-butylbromoacetate (0.61 g; 3.12 mmol) was added dropwise to the solution and stirred at room temperature overnight. The solution was concentrated under vacuum and purified via column chromatorgraphy (H/EA, 3:1; Rf = 0.32). The product **3** was obtained as yellow oil (0.66 g; 1.17 mmol; 49 %).
^{1}H-NMR (CDCl3, 400 MHz): 3.64 (s, 3 H); 3.28 (s, 4 H); 3.21 (s, 2 H); 2.77 (m, 4 H); 2.67 (m, 4 H); 2.30 (t, 3 H); 1.59(m, 2 H); 1.45 (s, 9 H); 1.44 (s, 18 H); 1.28 (m, 4 H); ^{13}C-NMR (CDCl3, 100 MHz): 174.25 (s), 171.97 (s), 171.09 (s), 81.05 (s), 80.96 (s), 63.58 (s), 62.12 (s), 58.10 (s), 57.46 (s), 51.58 (s), 44.78 (s), 35.34 (s), 34.18 (s), 28.36 (s), 28.27 (s), 25.86 (s), 22.73 (s) MS (ESI[+]): 572.34, 573.38, 574.41 (M+H^{+})

*1,4-Di(tert-butylacetate)-6-methylpentonate-6-(amino(methyl)-tert-butylacetate)-perhydro-1,4 diazepane (4)*: **3** (0,60 g; 1.05 mmol) was dissolved in acetonitrile (5 mL) and formaline solution (293 µL; 10.50 mmol) and acidified with acetic acid (180 µL; 3.15 mmol). The solution

was stirred for 15 minutes and sodium borohydride (0.12 g; 3.15 mmol) was added portionwise. After completion the solution was quenched with water, extracted with chloroform (3 x 10 mL) and the organic fractions were dried over sodium sulfate, filtrated and concentrated under vaccum. The crude product was purified via column chromatography (H/EA, 1:1; $R_f$ = 0.20). The product **4** was obtained as yellowish oil (0.50 g; 0.86 mmol; 82 %).

$^{1}$H-NMR (CDCl$_3$, 400 MHz):3.64 (s, 3 H); 3.46 (s, 2 H); 3.25 (m, 4 H); 2.94 (d, 2 H); 2.84-2.65 (m, 6 H); 2.31 (t, 2 H); 1.57 (m, 4 H); 1.45 (s, 18 H); 1.44 (s, 9 H); 1.35 (s, 2 H); $^{13}$C-NMR (CDCl$_3$, 100 MHz): 174.23, 172.17, 170.72, 80.90, 80.35, 77.34, 62.52, 62.34, 58.80, 53.99, 51.42, 37.34, 36.61, 34.09, 28.22, 28.12, 25.73, 21.91, MS (ESI$^+$): 586.34, 587.39, 588.43 (M+H$^+$)

*1,4-Di(acetate)-6-pentanoic acid-6-(amino(methyl)-acetate)-perhydro-1,4-diazepane (5)*: **4** (0.43 g; 0.72 mmol) was dissolved in 1,4-dioxane (10 mL), treated with 1M LiOH solution (3.8 mL; 3.80 mmol) and heated at 40 °C for 6 h. After completion the solution was concentrated, the residue was dissolved in a mixture of acetonitrile (0.5 mL), methanol (0.5 mL) and water (0.5 mL). The solution was treated with ice cold diethylether and the colourless precipitate was filtrated and purified via HPLC. The product **5** was obtained as colourless solid (58.0 mg; 0.14 mmol; 20 %; $t_R$ = 10.6 min (0 % to 30 % **B** in 20 min)).

$^{1}$H-NMR (D$_2$O, 400 MHz): 3.15 (s, 2 H); 3.10 (s, 4 H); 2.87-2.83 (d, J = 14.5 Hz, 2 H); 2.85-2.79 (m, 2 H); 2.71-2.68 (d, J = 14.8 Hz, 2 H); 2.58-2.52 (m, 2 H); 2.17 (s, 3 H); 2.13 (t, 2 H); 1.48-1.41 (m, 2H); 1.31-1.16 (m, 4 H); $^{13}$C-NMR (D$_2$O, 100 MHz): 182.53 (s); 180.32 (s); 66.68 (s); 64.94 (s); 62.24 (s); 56.19 (s); 38.75 (s); 36.58 (s); 31.53 (s); 28.61 (s); 25.29 (s); 24.04 (s); 15.24 (s)  MS (ESI$^+$): 404.2014, 405.2098, 406.2268 (M+H$^+$)
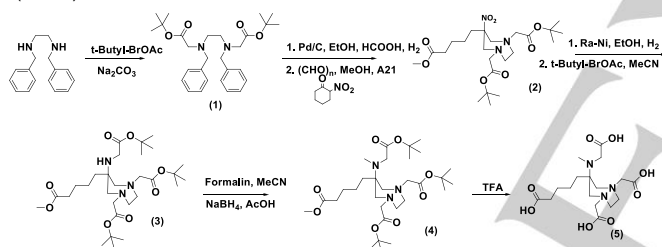


## 5. Equilibrium measurements

The protonation constants of DATA$^m$ and DATA$^{5m}$ ligands, the stability and protonation constants of Ca$^{II}$-, Mn$^{II}$- and Zn$^{II}$-complexes formed with DATA$^m$ and DATA$^{5m}$ ligands were determined by pH-potentiometric titration from acidic to basic pH range. The metal-to-ligand concentration ratios were 1:1 (the concentration of the ligands were generally 0.002 M). The stability and protonation constants of the "cold" Ga$^{III}$-complexes of DATA$^m$ and DATA$^{5m}$ were calculated from the pH-potentiometric titration of the Ga$^{3+}$ - L systems obtained from basic to acidic pH range by studying the competition reaction between DATA$^m$ or DATA$^{5m}$ and OH$^-$ for Ga$^{3+}$ ([L]=[Ga$^{3+}$]= 3×10$^{-3}$ M). The protonation constants of Cu(DATA$^m$)$^-$ and Cu(DATA$^{5m}$)$^{2-}$ were determined by pH-potentiometric titrations of CuL complex in the pH range of 1.7 – 11.7 ([CuL]= 2×10$^{-3}$ M). For pH measurements and pH-potentiometric titrations, a Metrohm 785 DMP Titrino titration workstation and a Metrohm-6.0233.100 combined electrode were used. The pH potentiometric titrations were performed at constant ionic strength (0.15 M NaCl) in 6 ml samples at 25 °C. The solutions were stirred, and N$_2$ was bubbled through them. The titrations were made in the pH range of 1.7-11.7. KH-phthalate (pH=4.005) and borax (pH=9.177) buffers were used to calibrate the pH meter. For the calculation of [H$^+$] from the measured pH values, the method proposed by Irving et al. was used. A 0.01M HCl solution was titrated with the standardized NaOH solution in the presence of 0.15 M NaCl ionic strength. The differences between the measured (pH$_{read}$) and calculated

pH (-log[H$^+$]) values were used to obtain the equilibrium H$^+$ concentration from the pH values, measured in the titration experiments. The ionic product of water (pK$_w$) at 25°C in 0.15 M NaCl was found to be 13.85.[30] The stability constant of Cu(DATA$^m$)$^-$ and Cu(DATA$^{5m}$)$^{2-}$ was determined by spectrophotometry in the [H$^+$] range of 0.01 – 1.0 M ([L]=[Cu$^{2+}$]= 2×10$^{-3}$ M). Seven samples were prepared and the H$^+$ concentration ([H$^+$]=0.010, 0.025, 0.050, 0.10, 0.32, 0.60 and 1.0 M) in the samples was adjusted with the addition of calculated amounts of 2.0 M HCl. The samples were kept at 25 °C for 7 days in order to attain the equilibrium (the time needed to reach the equilibrium was determined by spectrophotometry). The absorbance values of the samples were measured at 11 wavelengths (575, 595, 615, 635, 655, 675, 695, 715, 735, 755 and 775 nm). The ionic strength of samples with [H$^+$]=0.32, 0.60 and 1.0 M was not constant (the ionic strength of samples with [H$^+$]=0.010, 0.025, 0.050, 0.10 M was [H$^+$]+[Na$^+$]=0.15 M). For the equilibrium calculations, the molar absorptivities of the Cu$^{2+}$, CuL, CuHL, CuH$_2$L and CuH$_3$L species were used. The molar absorptivities of Cu$^{2+}$, Cu(DATA$^m$)$^-$ and Cu(DATA$^{5m}$)$^{2-}$ complexes were determined by recording the VIS spectra (λ=400 – 800 nm) of 1.0×10$^{-4}$, 2.0×10$^{-4}$, 3.0×10$^{-4}$ and 4.0×10$^{-4}$ M solutions in the pH range 1.7 – 7.0 (0.15 M NaCl, 25°C). The pH was adjusted by stepwise addition of concentrated NaOH or HCl. The spectrophotometric measurements were made with the use of a Cary 1E spectrophotometer at 25 °C, using 1.0 cm cells. The protonation and stability constants were calculated with the PSEQUAD program.[31]

## 6. NMR experiments

$^{1}$H- and $^{71}$Ga-NMR measurement were performed with a Bruker DRX 400 (9.4 T) equipped with a Bruker VT-1000 thermocontroller and a BB inverse z gradient probe (5 mm). The formation and protonation/deprotonation processes of the Ga(DATA$^m$) and Ga(DATA$^{5m}$)$^-$ were followed from basic to acidic pH range at 298K in 0.15 M NaCl. For these experiments, 0.008 M solution of the Ga(DATA$^m$) and Ga(DATA$^{5m}$) in H$_2$O was prepared (a capillary with D$_2$O was used for lock). The pH was adjusted with the addition of concentrated solution of NaOH and HCl. Because of the metal exchange between the Ga(DATA$^m$)OH or Ga(DATA$^{5m}$)OH and [Ga(OH)$_4$]$^-$ was in the "slow exchange regime" on the actual NMR timescale, the calculation of the logβ$_{GaLH-1}$ value of Ga(DATA$^m$)OH and Ga(DATA$^{5m}$)OH was performed by using the integrals of the $^{71}$Ga-NMR signal of [Ga(OH)$_4$]$^-$ complex. The molar integral values of $^{71}$Ga-NMR signal of [Ga(OH)$_4$]$^-$ complex were determined by recording the $^{71}$Ga NMR spectra of 0.01, 0.015, 0.02 and 0.025 M solutions of [Ga(OH)$_4$]$^-$ complex (pH=12.5, 0.15 M NaCl, 25°C). Calculation of the the logβ$_{GaLH-1}$ value was performed by the fitting of the integral – pH data pairs with the computer program *Micromath Scientist*, version 2.0 (Salt Lake City, UT, USA).

## 6. NMR experiments

The structural behavior and the dynamic processes of the Ga(DATA$^m$), Ga(DATA$^{5m}$)$^-$ and Ga(AAZTA)$^-$ complexes were followed by $^{1}$H-NMR spectroscopy. The Ga(DATA$^m$), Ga(DATA$^{5m}$)$^-$ and Ga(AAZTA)$^-$ complexes were prepared in D$_2$O ([Ga(DATA$^m$)]=0.015 M, ([Ga(DATA$^{5m}$)]=0.008 M and ([Ga(AAZTA)]=0.010 M). The pH of samples was adjusted by stepwise addition of NaOH and/or HCl. The chemical shifts are reported in ppm, with respect to DSS (4,4-dimethyl-4-silapentane-1-sulfonic acid) an external standard (0 ppm for the methyl protons of DSS).

## 7. Transmetallation kinetics

The rates of the exchange reactions taking place between Ga(DATA$^m$) or Ga(DATA$^{5m}$) and Cu$^{2+}$ in the presence of citrate were studied by spectrophotometry, following the formation of the Cu(DATA$^m$) or Cu(DATA$^{5m}$) complexes at 300 nm, with the use of 1.0 cm cells and a Cary 1E spectrophotometer. The concentration of Cu$^{2+}$ was 0.1 and 0.2

mM, while that of Ga<sup>III</sup>-complexes were 10 and 20 times higher, in order to ensure pseudo-first-order conditions. In order to prevent the hydrolysis of $Ga^{3+}$ and $Cu^{2+}$ ions, the transmetallation reactions were studied in the presence of citrate excess ([Cit]$_t$=2.0 mM). The exchange rates were studied in the pH range about 6.0 - 9.0. For keeping the pH values constant, MES (pH range 6.0 - 7.0), HEPES (pH range 7.0 - 8.5) and piperazine (pH range 8.5 - 9.0) buffers (0.01 M) were used. The temperature was maintained at 25°C and the ionic strength of the solutions was kept constant (0.15 M NaCl). The pseudo-first-order rate constants ($k_d$) were calculated from the tangent to the absorbance vs. time curves ($\Delta Abs/\Delta t$) with Eq. (12). For the calculations, the molar absorptivities of Cu(DATA$^m$), Cu(DATA$^{5m}$) and Cu(Cit)H$_{-1}$ were used, which were determined at 300 nm by recording the spectra of $1.0\times10^{-4}$, $2.0\times10^{-4}$, $3.0\times10^{-4}$ and $4.0\times10^{-4}$ M solutions in the pH range 5 - 10 (0.15 M KCl, 25°C). The calculations were performed with the use of the computer program *Micromath Scientist*, version 2.0 (Salt Lake City, UT, USA).

**8. Ligand-exchange kinetics with transferrin**
The ligand exchange reaction between Ga(DATA$^m$) or Ga(DATA$^{5m}$) and human serum transferrin (Sigma, partially $Fe^{3+}$ saturated) have been studied by spectrophotometry, following the formation of Ga(sTf) complex at 246 nm and pH=7.4 with the use of 1.0 cm cells and Cary 1E spectrophotometer. The concentration of the human serum transferrin solution was determined from the absorbance at 280 nm using the molar absorptivity $\varepsilon_{280}$=91200 cm$^{-1}$M$^{-1}$.[32] In order to ensure the pseudo-first-order condition, the rate of the ligand exchange reactions were studied in the presence of high excess of Ga<sup>III</sup>-complexes ([Ga(DATA$^m$)]=[Ga(DATA$^{5m}$)]=0.2 and 0.3 mM, [sTf]=10 µM)). The temperature was maintained at 25°C, the ionic strength and the hydrogen-carbonate concentration of the samples were kept constant; 0.15 M for NaCl and 0.025 M for NaHCO$_3$, respectively.

## Acknowledgements

**Keywords:** Ligands • Gallium • Molecular Imaging• Thermodynamic • Kinetics • Reaction mechanisms • NMR

[1] I. Velikyan, J. Label. *Compd. Radiopharm.* **2015**, 99–121
[2] M. Fani, J. P. André, H. R. Maecke, H. R. *Contrast Media Mol. Imaging* **2008**, *3* (2), 53.
[3] A. Vértes, S. Nagy, Z. Klencsár, G. L. Rezsó, F. Roesch, *Radionuclide Generators*, 2 nd.; Springer, Ed.; **2011**.
[4] a) I. Velikyan, *Molecules* **2015**, *20*, 12913-12943; b) I. Velikyan, *Theranostics* **2014**, *4*, 47-80.
[5] a) T. J. Wadas, E. H. Wong, G. R. Weisman, C. J. Anderson, *Chem. Rev.* **2010**, *110*, 2858–2902; b) F. Rösch, *Appl. Radiat. Isot.* **2013**, *76*, 24–30.
[6] a) W. R. Harris, A. E. Martell, *Inorg. Chem.*, **1976**, *15*, 713-720.; b) R. J. Motekaitis, A. E. Martell, *Inorg. Chem.*, **1980**, *19*, 1646-1651.
[7] a) E. W. Price, C. Orvig, *Chem. Soc. Rev.*, **2014**, *43*, 260-290; b) A. S. Craig, H. Adams, N. R. Bailey, D. Parker , *J. Chem. Soc., Chem. Commun.* **1989**, 1793-1794; c) J. P.L. Cox, A.S. Craig, I.M. Helps, K.J. Jankowski, D. Parker, M.A.W. Eaton, A.T. Millican, K. Millar, N.R.A.

[8] Beeley and B.A. Boyce, *J. Chem. Soc., Perkin Trans I*, **1990**, 2567-2577
[8] a) J. Notni, P. Hermann, J. Havlickova, J. Kotek, V. Kubicek, J. Plutnar, N. Loktinova, P. J. Riss, F. Rösch, I. Lukes, *Chem. Eur. J.*, **2010**, *16*, 7174 – 7185; b) J. Notni, J. Simecek, P. Hermann, H. J. Wester, *Chem. Eur. J.* **2011**, *17*, 14718–14722; c) J. Simecek, M. Schulz, J. Notni, J. Plutnar, V. Kubicek, J. Havlickova, P. Hermann, *Inorg. Chem.* **2012**, *51*, 577–590.
[9] a) I. Velikyan, H. Maecke, B. Langstrom, *Bioconjugate Chem.* **2008**, *19*, 569–573; b) D. J. Berry, Y. Ma, J. R. Ballinger, R. Tavare, A. Koers, K. Sunassee, T. Zhou, S. Nawaz, G. E. D. Mullen, R. C. Hider, P. J. Blower, *Chem. Commun.* **2011**, *47*, 7068-7070.
[10] a) S. Aime, L. Calabi, C. Cavallotti, E. Gianolio, G. B. Giovenzana, P. Losi, A. Maiocchi, G. Palmisano, M. Sisti, *Inorg. Chem.* **2004**, *43*, 7588-7590. b) G. Gugliotta, M. Botta, G. B. Giovenzana, L. Tei, *Bioorg. Med. Chem. Lett.* **2009**, *19*, 3442-3444.
[11] Zs. Baranyai, F. Uggeri, G. B. Giovenzana, A. Bényei, E. Brücher, S. Aime, *Chem. Eur. J.* **2009**, *15*, 1696-1705.
[12] Z. Baranyai, F. Uggeri, A. Maiocchi, G. B. Giovenzana, C. Cavallotti, A. Takács, I. Tóth, I. Bányai, A. Bényei, E. Brucher, S. Aime, *Eur. J. Inorg. Chem.*, **2013**, 147 – 162.
[13] G. Nagy, D. Szikra, Gy. Trencsényi, A. Fekete, I. Garai, A. M. Giani, R. Negri, N. Masciocchi, A. Maiocchi, F. Uggeri, I. Tóth, S. Aime, G. B. Giovenzana, Zs. Baranyai, *Angew. Chem. Int. Ed.*, **2017**, *56*, 2118–2122.
[14] A. Vágner, C. D'Alessandria, G. Gambino, M. Schwaiger, S. Aime, A. Maiocchi, I. Tóth, Zs. Baranyai, L. Tei, *ChemistrySelect* **2016**, *1*, 163-171.
[15] K. C. Briley-Saebo, S. Geninatti, A. Barazza, D. Cormode, W. J. M. Mulder, W. Chen, G. B. Giovenzana, S. Aime, Z. A. Fayad, *J. Phys. Chem. B* **2009**, *113*, 6283-6289.
[16] E. Gianolio, G. B. Giovenzana, A. Ciampa, S. Lanzardo, D. Imperio, S. Aime, *Chem. Med. Chem.* **2008**, *3*, 60-62.
[17] G. Gugliotta, M. Botta, G. B. Giovenzana, L. Tei, *Bioorg. Med. Chem. Lett.* **2009**, *19*, 3442-3444.
[18] L. Manzoni, L. Belvisi, D. Arosio, M. P. Bartolomeo, A. Bianchi, C. Brioschi, F. Buonsanti, C. Cabella, C. Casagrande, M. Civera, M. De Matteo, L. Fugazza, L. Lattuada, F. Maisano, L. Miragoli, C. Neira, M. Pilkington-Miksa, C. Scolastico, *ChemMedChem* **2012**, *7*, 1084 – 1093.
[19] B. P. Waldron, D. Parker, C. Burchardt, D. S. Yufit, M. Zimny, F. Roesch, *Chem. Commun.*, **2013**, *42*, 579-581
[20] a) D. Parker, B. P. Waldron, *Org. Biomol. Chem.*, **2013**, *11*, 2827 – 2838; b) B. P. Waldron , D. Parker, D. S. Yufit, *Dalton Trans.* **2013**, *42*, 8001-8008.
[21] a) J. Seemann, B. P. Waldron, F. Roesch, D. Parker, *ChemMedChem* **2015**, *10*, 1019; b) J. Seemann, B. P. Waldron, D. Parker and F. Roesch *EJNMMI Radiopharmacy and Chemistry* **2016**, *1*, 1-12.
[22] L. Tei, G. Gugliotta, M. Fekete, F. K. Kálmán, M. Botta, *Dalton Trans.*, **2011**, *40*, 2025.
[23] L. Barcza, K. Mihályi, *Z. Phys. Chem.*, **1977**, *104*, 199.
[24] C. F. Baes, R. E. Mesmer, *The Hydrolysis of Cations*, Wiley, New York, **1976**.
[25] J. W. Akitt, D. Kettle, *Mag. Res. Chem.*, **1989**, *27*, 377 –379.
[26] I. Tóth, L. Zékány, E. Brücher, *Polyhedron*, **1984**, *3*, 871 – 877.
[27] V. Kubicek, J. Havlivkova, J. Kotek, G.Tircsó, P. Hermann, É. Tóth, I. Lukes, *Inorg. Chem.* **2010**, *49*, 10960–10969.
[28] a) G. E. Jackson, M. J. Byrne, *J. Nucl. Med.* **1996**, *37*, 379.; b) P. M. May, D. R. Williams, P. W. Linder, *J. Chem. Soc. Dalton Trans.*, **1977**, 588 - 595
[29] W. R. Harris, V. L. Pecoraro, *Biochemistry*, **1983**, *22*, 292 – 299.
[30] H. M. Irving, G. M. Miles, D. L. Pettit, *Anal. Chim. Acta*, **1967**, *38*, 475-482.

[31]   L. Zékány, I. Nagypál in '*Computational Method for Determination of Formation Constants*' Ed. D. J. Legett, Plenum, New York, **1985**, p. 291.

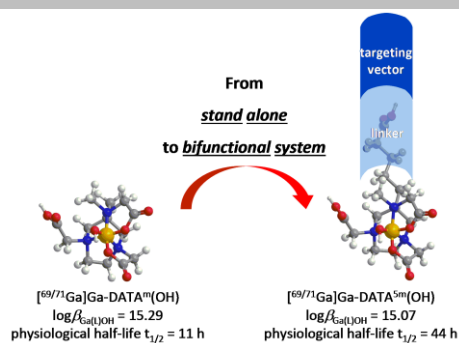[32]   H. N. Takahashi, E. Doi, M. Hirose, *J. Biochem*, **1989**, *106*, 858 – 863.

**Entry for the Table of Contents**

# FULL PAPER

Text for Table of Contents

MUST BE INSERTED

From
_stand alone_
to _bifunctional system_

[69/71Ga]Ga-DATA$^m$(OH)
$\log \beta_{Ga(L)OH} = 15.29$
physiological half-life $t_{1/2} = 11$ h

[69/71Ga]Ga-DATA$^{5m}$(OH)
$\log \beta_{Ga(L)OH} = 15.07$
physiological half-life $t_{1/2} = 44$ h

_E. Farkas, J. Nagel, A. Maiocchi, B. P. Waldron, D. Parker, I. Tóth, E. Brücher F. Roesch* and Zs. Baranyai*_

**_Page No. – Page No._**

**Equilibrium, kinetic and structural properties of gallium(III)- and some divalent metal complexes formed with the new DATA$^m$ and DATA$^{5m}$ ligands**